[86] X. J. Xu, J. X. Hao, H. Aldskogius, A. Seiger, and Z. Wiesenfeld-Hallin, "Chronic pain-related syndrome in rats after ischemic spinal cord lesion: a possible animal model for pain in patients with spinal cord injury," *Pain*, vol. 48, no. 2, pp. 279–290, 1992.

[87] R. Prado, W. D. Dietrich, B. D. Watson, M. D. Ginsberg, and B. A. Green, "Photochemically induced graded spinal cord infarction. Behavioral, electrophysiological, and morphological correlates," *Journal of Neurosurgery*, vol. 67, no. 5, pp. 745–753, 1987.

[88] M. Gaviria, H. Haton, F. Sandillon, and A. Privat, "A mouse model of acute ischemic spinal cord injury," *Journal of Neurotrauma*, vol. 19, no. 2, pp. 205–221, 2002.

[89] J. X. Hao, T. Stöhr, N. Selve, Z. Wiesenfeld-Hallin, and X. J. Xu, "Lacosamide, a new anti-epileptic, alleviates neuropathic pain-like behaviors in rat models of spinal cord or trigeminal nerve injury," *European Journal of Pharmacology*, vol. 553, no. 1-3, pp. 135–140, 2006.

[90] M. von Heijne, J. X. Hao, A. Sollevi, and X. J. Xu, "Effects of intrathecal morphine, baclofen, clonidine and R-PIA on the acute allodynia-like behaviours after spinal cord ischaemia in rats," *European Journal of Pain*, vol. 5, no. 1, pp. 1–10, 2001.

[91] J. X. Hao, X. J. Xu, H. Aldskogius, A. Seiger, and Z. Wiesenfeld-Hallin, "Photochemically induced transient spinal ischemia induces behavioral hypersensitivity to mechanical and cold stimuli, but not to noxious-heat stimuli, in the rat," *Experimental Neurology*, vol. 118, no. 2, pp. 187–194, 1992.

[92] W. P. Wu, J. X. Hao, X. J. Xu, Z. Wiesenfeld-Hallin, W. Koek, and F. C. Colpaert, "The very-high-efficacy 5-HT receptor agonist, F 13640, preempts the development of allodynia-like behaviors in rats with spinal cord injury," *European Journal of Pharmacology*, vol. 478, no. 2-3, pp. 131–137, 2003.

[93] J. X. Hao, X. J. Xu, Y. X. Yu, A. Seiger, and Z. Wiesenfeld-Hallin, "Transient spinal cord ischemia induces temporary hypersensitivity of dorsal horn wide dynamic range neurons to myelinated, but not unmyelinated, fiber input," *Journal of Neurophysiology*, vol. 68, no. 2, pp. 384–391, 1992.

[94] J. X. Hao, X. J. Xu, Y. X. Yu, A. Seiger, and Z. Wiesenfeld-Hallin, "Hypersensitivity of dorsal horn wide dynamic range neurons to cutaneous mechanical stimuli after transient spinal cord ischemia in the rat," *Neuroscience Letters*, vol. 128, no. 1, pp. 105–108, 1991.

[95] D. M. Basso, M. S. Beattie, and J. C. Bresnahan, "A sensitive and reliable locomotor rating scale for open field testing in rats," *Journal of Neurotrauma*, vol. 12, no. 1, pp. 1–21, 1995.

[96] K. Gale, H. Kerasidis, and J. R. Wrathall, "Spinal cord contusion in the rat: behavioral analysis of functional neurologic impairment," *Experimental Neurology*, vol. 88, no. 1, pp. 123–134, 1985.

[97] C. A. Fairbanks, K. L. Schreiber, K. L. Brewer et al., "Agmatine reverses pain induced by inflammation, neuropathy, and spinal cord injury," *Proceedings of the National Academy of Sciences of the United States of America*, vol. 97, no. 19, pp. 10584–10589, 2000.

[98] R. P. Yezierski, S. Liu, G. L. Ruenes, K. J. Kajander, and K. L. Brewer, "Excitotoxic spinal cord injury: behavioral and morphological characteristics of a central pain model," *Pain*, vol. 75, no. 1, pp. 141–155, 1998.

[99] P. Siddall, C. L. Xu, and M. Cousins, "Allodynia following traumatic spinal cord injury in the rat," *NeuroReport*, vol. 6, no. 9, pp. 1241–1244, 1995.

[100] M. G. Fehlings and C. H. Tator, "The relationships among the severity of spinal cord injury, residual neurological function, axon counts, and counts of retrogradely labeled neurons after experimental spinal cord injury," *Experimental Neurology*, vol. 132, no. 2, pp. 220–228, 1995.

[101] R. Nashmi and M. G. Fehlings, "Changes in axonal physiology and morphology after chronic compressive injury of the rat thoracic spinal cord," *Neuroscience*, vol. 104, no. 1, pp. 235–251, 2001.

[102] J. C. Bruce, M. A. Oatway, and L. C. Weaver, "Chronic pain after clip-compression injury of the rat spinal cord," *Experimental Neurology*, vol. 178, no. 1, pp. 33–48, 2002.

[103] S. A. Marques, V. F. Garcez, E. A. Del Bel, and A. M.B. Martinez, "A simple, inexpensive and easily reproducible model of spinal cord injury in mice: morphological and functional assessment," *Journal of Neuroscience Methods*, vol. 177, no. 1, pp. 183–193, 2009.

[104] A. D. Kloos, L. C. Fisher, M. R. Detloff, D. L. Hassenzahl, and D. M. Basso, "Stepwise motor and all-or-none sensory recovery is associated with nonlinear sparing after incremental spinal cord injury in rats," *Experimental Neurology*, vol. 191, no. 2, pp. 251–265, 2005.

[105] L. B. Jakeman, Z. Guan, W. Ping et al., "Traumatic spinal cord injury produced by controlled contusion in mouse," *Journal of Neurotrauma*, vol. 17, no. 4, pp. 299–319, 2000.

[106] T. Ito, S. Ohtori, G. Inoue et al., "Glial phosphorylated p38 MAP kinase mediates pain in a rat model of lumbar disc herniation and induces motor dysfunction in a rat model of lumbar spinal canal stenosis," *Spine*, vol. 32, no. 2, pp. 159–167, 2007.

[107] M. Sekiguchi, S. Kikuchi, and R. R. Myers, "Experimental spinal stenosis: relationship between degree of cauda equina compression, neuropathology, and pain," *Spine*, vol. 29, no. 10, pp. 1105–1111, 2004.

[108] G. Wang and S. M. Thompson, "Maladaptive homeostatic plasticity in a rodent model of central pain syndrome: thalamic hyperexcitability after spinothalamic tract lesions," *The Journal of Neuroscience*, vol. 28, no. 46, pp. 11959–11969, 2008.

[109] S. R. Chaplan, F. W. Bach, J. W. Pogrel, J. M. Chung, and T. L. Yaksh, "Quantitative assessment of tactile allodynia in the rat paw," *Journal of Neuroscience Methods*, vol. 53, no. 1, pp. 55–63, 1994.

[110] T. L. Yaksh, "Behavioral and autonomic correlates of the tactile evoked allodynia produced by spinal glycine inhibition: effects of modulatory receptor systems and excitatory amino acid antagonists," *Pain*, vol. 37, no. 1, pp. 111–123, 1989.

[111] G. J. Bennett and Y. K. Xie, "A peripheral mononeuropathy in rat that produces disorders of pain sensation like those seen in man," *Pain*, vol. 33, no. 1, pp. 87–107, 1988.

[112] Y. Choi, Y. W. Yoon, H. S. Na, S. H. Kim, and J. M. Chung, "Behavioral signs of ongoing pain and cold allodynia in a rat model of neuropathic pain," *Pain*, vol. 59, no. 3, pp. 369–376, 1994.

[113] D. M. Basso, L. C. Fisher, A. J. Anderson, L. B. Jakeman, D. M. McTigue, and P. G. Popovich, "Basso mouse scale for locomotion detects differences in recovery after spinal cord injury in five common mouse strains," *Journal of Neurotrauma*, vol. 23, no. 5, pp. 635–659, 2006.

[114] M. Martinez, J. M. Brezun, L. Bonnier, and C. Xerri, "A new rating scale for open-field evaluation of behavioral recovery after cervical spinal cord injury in rats," *Journal of Neurotrauma*, vol. 26, no. 7, pp. 1043–1053, 2009.

[115] J. C. Gensel, C. A. Tovar, F. P. T. Hamers, R. J. Deibert, M. S. Beattie, and J. C. Bresnahan, "Behavioral and histological characterization of unilateral cervical spinal cord contusion

injury in rats," *Journal of Neurotrauma*, vol. 23, no. 1, pp. 36–54, 2006.

[116] J. A. Bertelli and J.-C. Mira, "Behavioral evaluating methods in the objective clinical assessment of motor function after experimental brachial plexus reconstruction in the rat," *Journal of Neuroscience Methods*, vol. 46, no. 3, pp. 203–208, 1993.

[117] Y. Liu, D. Kim, B. T. Himes et al., "Transplants of fibroblasts genetically modified to express BDNF promote regeneration of adult rat rubrospinal axons and recovery of forelimb function," *The Journal of Neuroscience*, vol. 19, no. 11, pp. 4370–4387, 1999.

[118] A. A. Webb and G. D. Muir, "Sensorimotor behaviour following incomplete cervical spinal cord injury in the rat," *Behavioural Brain Research*, vol. 165, no. 2, pp. 147–159, 2005.

[119] J. F. Ditunno, J. W. Little, A. Tessler, and A. S. Burns, "Spinal shock revisited: a four-phase model," *Spinal Cord*, vol. 42, no. 7, pp. 383–395, 2004.

[120] F. Biering-Sørensen, J. B. Nielsen, and K. Klinge, "Spasticity-assessment: a review," *Spinal Cord*, vol. 44, no. 12, pp. 708–722, 2006.

[121] F. M. Maynard, R. S. Karunas, and W. P. Waring III, "Epidemiology of spasticity following traumatic spinal cord injury," *Archives of Physical Medicine and Rehabilitation*, vol. 71, no. 8, pp. 566–569, 1990.

[122] P. Boulenguez and L. Vinay, "Strategies to restore motor functions after spinal cord injury," *Current Opinion in Neurobiology*, vol. 19, no. 6, pp. 587–600, 2009.

[123] Y. Li, M. A. Gorassini, and D. J. Bennett, "Role of persistent sodium and calcium currents in motoneuron firing and spasticity in chronic spinal rats," *Journal of Neurophysiology*, vol. 91, no. 2, pp. 767–783, 2004.

[124] R. Katz, "Presynaptic inhibition in humans: a comparison between normal and spastic patients," *Journal of Physiology*, vol. 93, no. 4, pp. 379–385, 1999.

[125] G. I. Boorman, R. G. Lee, W. J. Becker, and U. R. Windhorst, "Impaired "natural reciprocal inhibition" in patients with spasticity due to incomplete spinal cord injury," *Electroencephalography and Clinical Neurophysiology*, vol. 101, no. 2, pp. 84–92, 1996.

[126] S. A. Edgley and N. C. Aggelopoulos, "Short latency crossed inhibitory reflex actions evoked from cutaneous afferents," *Experimental Brain Research*, vol. 171, no. 4, pp. 541–550, 2006.

[127] P. Boulenguez, S. Liabeuf, R. Bos et al., "Down-regulation of the potassium-chloride cotransporter KCC2 contributes to spasticity after spinal cord injury," *Nature Medicine*, vol. 16, no. 3, pp. 302–307, 2010.

[128] S. Hou, H. Duale, and A. G. Rabchevsky, "Intraspinal sprouting of unmyelinated pelvic afferents after complete spinal cord injury is correlated with autonomic dysreflexia induced by visceral pain," *Neuroscience*, vol. 159, no. 1, pp. 369–379, 2009.

J Anesth (2011) 25:523–530
DOI 10.1007/s00540-011-1173-9

ORIGINAL ARTICLE

Human brain activity associated with painful mechanical stimulation to muscle and bone

Lynn Maeda · Mayu Ono · Tetsuo Koyama · Yoshitetsu Oshiro · Masahiko Sumitani · Takashi Mashimo · Masahiko Shibata

Received: 8 February 2010 / Accepted: 12 May 2011 / Published online: 2 June 2011

Abstract
Purpose The purpose of this study was to elucidate the central processing of painful mechanical stimulation to muscle and bone by measuring blood oxygen level-dependent signal changes using functional magnetic resonance imaging (fMRI).
Methods Twelve healthy volunteers were enrolled. Mechanical pressure on muscle and bone were applied at the right lower leg by an algometer. Intensities were adjusted to cause weak and strong pain sensation at either target site in preliminary testing. Brain activation in response to mechanical nociceptive stimulation targeting muscle and bone were measured by fMRI and analyzed.
Results Painful mechanical stimulation targeting muscle and bone activated the common areas including bilateral insula, anterior cingulate cortex, posterior cingulate cortex, secondary somatosensory cortex (S2), inferior parietal lobe, and basal ganglia. The contralateral S2 was more activated by strong stimulation than by weak stimulation. Some areas in the basal ganglia (bilateral putamen and caudate nucleus) were more activated by muscle stimulation than by bone stimulation.
Conclusions The putamen and caudate nucleus may have a more significant role in brain processing of muscle pain compared with bone pain.

Keywords Pain · Muscle · Bone · Neuroimaging · fMRI

L. Maeda
Department of Anesthesia and Pain Medicine, Nishinomiya Municipal Central Hospital, Nishinomiya, Japan

L. Maeda · T. Mashimo
Department of Anesthesiology and Intensive Care Medicine, Osaka University Graduate School of Medicine, Suita, Japan

M. Ono
Department of Anesthesia, Ikeda City Hospital, Ikeda, Japan

T. Koyama
Department of Rehabilitation, Kyoritsu Neurosurgery Hospital, Nishinomiya, Japan

Y. Oshiro
Himeji Ishikawa Functional Brain Imaging Laboratory, Himeji, Japan

M. Sumitani
Department of Anesthesiology and Pain Relief Center, The University of Tokyo Hospital, Tokyo, Japan

M. Shibata (✉)
Department of Pain Medicine, Osaka University Graduate School of Medicine, 2-2 Yamadaoka, Suita, Osaka 565-0871, Japan
e-mail: mshibata@pain.med.osaka-u.ac.jp

Introduction

Physical pain originating from deep tissues—including sprains, fibromyalgia, rheumatic polymyalgia, and other muscle-derived pain, and bone-derived pain such as fractures, spondylosis, and bone tumors—is very commonly encountered. Consequently, understanding how these conditions come to be painful through brain processing is clinically important. Recent imaging research using the blood oxygen level-dependent-based (BOLD) functional magnetic resonance imaging (fMRI) method successfully revealed cognitive mechanisms in response to painful stimulation.

In the field of anesthesiology, fMRI has been on trial as a tool for investigating cerebral pain processing [1–5]. Previous reports, however, have mainly been studies of

heat stimulation to skin [6, 7]. More recently, studies targeting brain activation when muscle pain is caused using electric stimulation or hypertonic saline have successfully demonstrated that some areas are differently activated, including the contralateral primary somatosensory cortex (S1), the ipsilateral anterior insula, the contralateral motor cortex, the cingulate motor area, and the perigenual cingulate [8–10]. However, there are few studies of the brain processing activated by mechanical stimulation to deep tissues [11]. To elucidate the central processing of painful mechanical stimulation to deep tissues (muscle and bone), we compared the brain activation induced by two different intensities of stimulation (strong and weak) at two different targets (muscle and bone), using fMRI.

Materials and methods

Subjects

All the procedures were approved by the Osaka University Hospital Institutional Review Board. Twelve healthy volunteers (7 men, 5 women; aged 24–56 years) agreed to receive painful stimulation while their brain activation was evaluated. They had no neurological disorders or detectable MRI abnormalities in the brain and were free from any medication within 24 h before the study. In written informed consent, each acknowledged that they were willing to receive experimental painful stimulation. Before the protocols were carried out, each volunteer was familiarized with the experimental protocol, the types of stimulation, and the tasks performed.

Painful stimulation

To determine suitable stimulation intensities for each subject, a preliminary testing was performed immediately before the fMRI study. Perpendicularly applying a round 10-mm solid tip of an algometer probe (Pressure Algometer NPA-1, Shinko, Japan) on the surface (skin) at the medial point of the right tibia (Fig. 1), the experimenter gradually increased the pressure until the subject verbally indicated that the stimulation was painful. At that point, the pain intensity was taken to be '3' on a subjective 10-point numerical rating scale (NRS). The three median values of five trials were averaged to determine the weak stimulation to be applied to the tibia of particular volunteers. Similarly, the subject was asked to verbally indicate when the pain was such that it would probably be intolerable for more than 20 s without withdrawal movement. At this point, pain intensity was scored as '8' on the volunteer's subjective 10-point NRS. Similar grading of muscle pain was also carried out [12]. Here the tip of the probe was applied to the skin on the gastrocnemius muscle at a medial point 3–5 cm from the stimulation point of the tibia (Fig. 1). For each volunteer, as in the bone protocol, subjective NRS pain scores of '3' and '8' were obtained. These procedures were conducted by one experimenter (M.S.) who, in each instance and so far as possible, endeavored to consistently apply the required level of pressure perpendicularly.

Protocol

Each subject participated in a trial comprising 12 fMRI task sessions. At each right-leg site that was evaluated in the preliminary testing, three trials of 20 s of strong or weak stimulation were applied in each session. The site and strength of stimulation were pseudo random for each series. After each series of three stimulations (in a session lasting 3 min; Fig. 2), there was a pause of 1 min before the next session. MRI scans were acquired throughout the 36-min period. The subjects were asked to rate, using NRS, the overall pain at the end of each series of three stimulations (mean of three periods of 20-s stimulation). Before the

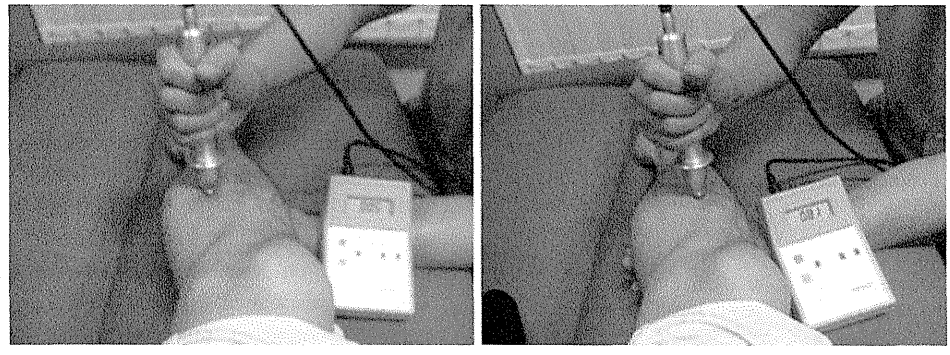

Fig. 1 Photograph showing how a digital algometer was used to apply stimulation to muscle (*left*) and bone (*right*). Bone stimulation was applied to the surface (skin) at the midpoint of tibia. Muscle stimulation was applied to the surface of gastrocnemius 3–5 cm posterior from bone stimulation point. Intensities of stimulation (muscle vs. bone, strong vs. weak) were decided for each subject by averaging the values of the median of three of five trials

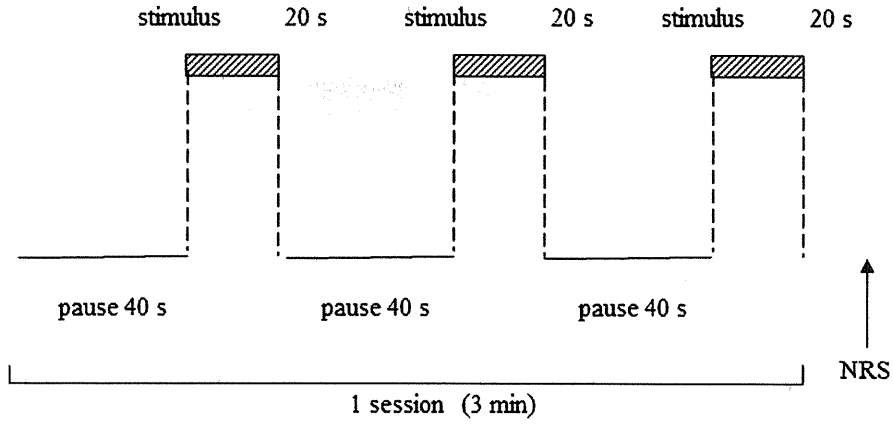

Fig. 2 Schematic representation of the experiment. Each subject underwent one trial comprising 12 sessions with a 1-min interval between sessions. Each session, lasting a total of 3 min, started with 40-s pause, and then a 20-s strong or weak stimulation to either muscle or bone. Weak and strong stimulations for each volunteer were decided in the preliminary testing. The order of stimulation was pseudo randomized. After each session, volunteers were asked to score the perceived pain. *NRS* numerical rating scale

commencement of the protocol, each volunteer was informed that the site (muscle or bone) and intensity (weak or strong) of the forthcoming series of stimulation would be random.

MRI

Imaging was performed with a 1.5-T MRI scanner (Signa EXCITE XI 11.0; GE Healthcare, Milwaukee, WI, USA). Functional MR images were obtained using a multislice echo planar imaging technique (EPI) based on 30 oblique slices (repetition time, 3,000 ms; time to echo, 60 ms; flip angle, 90°; slice thickness, 5 mm; gap, 0 mm; field of view, 300 mm × 300 mm; in-plane resolution, 4.69 mm × 4.69 mm). All the subjects were positioned in the scanner with a foam rubber pad to minimize head movement and instructed simply to lie with their eyes closed without moving or speaking. Their heads were placed so that the uppermost superior aspect of brain was within the field of view. High-resolution T_1-weighted anatomic images with the same orientation as the EPI slices were collected from each subject. In the subsequent analysis, these images were used for coregistration of functional and anatomic data.

Data analysis

Psychophysics

Using paired *t* testing, we compared the stimulation intensity and the average subjective NRS scores for muscle (weak and strong) and bone (weak and strong), respectively. Effects of order of stimulus application on NRS were evaluated with two-way analysis of variance (ANOVA); $P < 0.05$ was regarded as significant. Values are given as mean ± SD.

fMRI data analysis

The fMRI data were analyzed with Statistical Parametric Mapping software (SPM99; Wellcome Department of Cognitive Neurology, London, UK) implemented in Matlab 6.1 (Mathworks, Sherborn, MA, USA). The functional images were realigned to correct for head movements, coregistered with each subject's anatomic MRI, and transformed to the format of the standard brain according to Talairach coordinates [13]. The functional images were spatially smoothed with an 8-mm full-width half-maximum Gaussian kernel. We fitted a linear regression model (fixed effects within subjects). Each condition was modeled with a boxcar function and convolved with a hemodynamic response function. Temporally, the voxel time series were high-pass filtered (124-s cutoff periods) to remove slow trends in the data, and low-pass filtered with a hemodynamic response filter.

We compared image data for each group—weak muscle stimulation, strong muscle stimulation; weak bone stimulation, strong bone stimulation—against the data from each resting condition, respectively. All the data were pooled for group statistical comparisons. Across the subjects, random effect analysis was performed to determine the significant activation associated with different sites and intensities of stimulation ($P < 0.001$ uncorrected; minimum cluster size, 20 voxels). To investigate the brain network related to painful stimulation intensity, we calculated the difference in the areas activated by strong stimulation minus weak stimulation (paired *t* test; $P < 0.005$ uncorrected; minimum cluster size, 20 voxels). To identify the brain areas that are differently activated by muscle and bone stimulation, we also analyzed the data separately (strong muscle minus strong bone; weak muscle minus weak bone; and all

together) (paired t test; $P < 0.005$ uncorrected; minimum cluster size, 20 voxels).

Results

Stimulation and pain intensity

The mean intensity of muscle stimulation was 21.1 ± 8.4 N for weak stimulation and 40.7 ± 7.8 N for strong stimulation; the mean intensity of bone stimulation was 14.2 ± 5.7 N for weak stimulation and 30.1 ± 7.9 N for strong stimulation. The NRS scores with strong muscle and strong bone stimulation were significantly higher than those with weak muscle and weak bone stimulation, respectively ($P < 0.05$ for both) (Table 1). All the volunteers clearly distinguished the two intensities of stimulation because the weaker stimulation was always scored lower. Although the volunteers found weak muscle stimulation trials more painful ($P < 0.05$) than weak bone stimulation, no similar difference was found for strong stimulations. Comparing the data among the three trials of the same intensity at the same site, no differences in NRS scores were found; this indicates that repeated mechanical stimulation did not sensitize or desensitize the volunteers ($P > 0.05$).

fMRI

In response to painful muscle stimulation, brain activation was apparent within the bilateral anterior cingulate cortex (ACC), insula cortex, the secondary somatosensory cortex (S2), the inferior parietal lobule (IPL), the posterior cingulate cortex (PCC), putamen, the ipsilateral dorsolateral prefrontal cortex (DLPFC), thalamus, caudate, and the contralateral claustrum (Fig. 3a,b; Table 2). In response to painful bone stimulation, brain activation was also apparent within the bilateral ACC, the IPL, the S2, the PCC, the ipsilateral DLPFC, and the contralateral claustrum (Fig. 4a,b; Table 2). Peak coordinates (x, y, z) in Montreal Neurological Institute (MNI) space and Z-scores (>6.00) for the activated brain regions by muscle and bone pain are shown in Table 2. Differences in the areas activated by strong versus weak muscle stimulation were mainly found in the contralateral S2 and the bilateral thalamus (Fig. 3c). For strong versus weak bone stimulation, the difference was found in the contralateral S2 (Fig. 4c). With weak stimulations, the activation differences between muscle and bone stimulation were apparent in the bilateral caudate nucleus and contralateral Brodmann areas 22 and 45 (Fig. 5a). With strong stimulations, the activation differences were apparent in the bilateral putamen, the ipsilateral ACC, and the contralateral claustrum (Fig. 5b). Analyzing the sum of the differences between muscle- and bone-related pain revealed that activation was different in the bilateral caudate and contralateral putamen (Fig. 5c; Table 3).

Discussion

In this study, as an initial step toward elucidating the brain activation associated with mechanically induced deep tissue pain, we found that the contralateral S2 was more activated by stronger stimulations to muscle or bone. We also found that parts of the basal ganglia (putamen and caudate nucleus) were more activated by muscle stimulation than by bone stimulation.

Psychophysics

The NRS scores measured during fMRI were higher than those determined in the preliminary testing. Although the reason is not clear, the difference of the rate of pressure increase between preliminary testing and the fMRI session may be a cause.

On the other hand, the NRS scores for the two sets of three stimulations at each site did not change during the protocol (see Table 1), suggesting that no further change in sensitivity occurred. Nie et al. [14] have reported that after

Table 1 Numerical rating scale (0–10 NRS) by mechanical stimulation

	1st stimulation	2nd stimulation	3rd stimulation	mean
weak muscle stimulation	4.83±1.99	4.67±1.88	4.5±1.98	4.67±1.90
strong muscle stimulation	8.17±1.34	8.5±1.17	8.25±1.42	8.31±1.28
weak bone stimulation	4.25 ±2.14	3.25 ±1.14	3.92 ±1.78	3.81±1.74
strong bone stimulation	8.83 ±1.03	8.25 ±1.36	8.17 ±1.70	8.42 ±1.38

NRS with strong muscle and strong bone stimulation were significantly higher than those with weak muscle and weak bone stimulation (*$P < 0.05$). In weak stimulations, NRS with muscle stimulation was higher than with bone stimulation (**$P < 0.05$). There were no differences between strong muscle and bone stimulations among NRS with 1st, 2nd, and 3rd stimulation in the same study groups

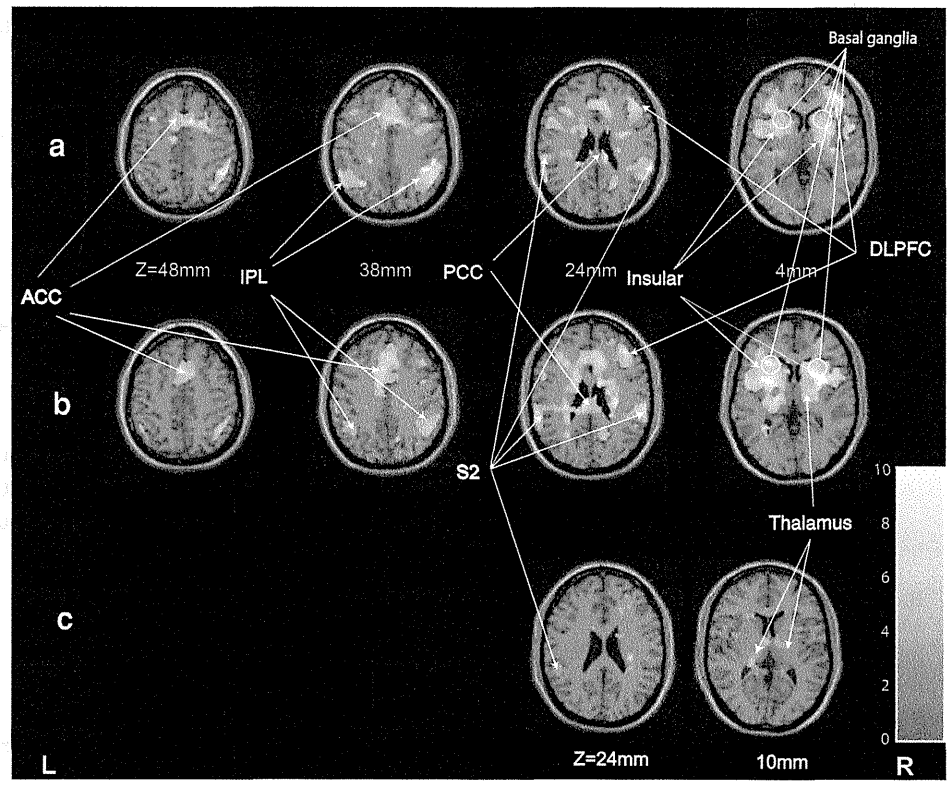

Fig. 3 Brain activation induced by muscle stimulation: weak stimulation (**a**), strong stimulation (**b**), and contrast of strong and weak stimulation (**c**). In millimeter elevations relative to a line through the anterior–posterior commissure (AC–PC line), brain slices are shown in superior–inferior sequence. The axial slices are arranged from dorsal (*left*) to ventral (*right*). Statistical map thresholds are $P < 0.001$ (**a**, **b**, uncorrected), and $P < 0.005$ (**c**, uncorrected, paired test). Minimum cluster size is 20 voxels. Right (*R*) and left (*L*) sides are indicated. *ACC* anterior cingulate cortex; *IPL* inferior parietal lobule; *S2* secondary sensory cortex; *DLPFC* dorsolateral prefrontal cortex; *PCC* posterior cingulate cortex

ten stimulations with 30-s intervals between stimulations, subjects gave higher VAS scores, increasing to 192% ± 71% for stimulation of the tibia and to 117% ± 42% for stimulation of the tibia anterior muscle. In the present study, the protocol specified a 60-s interval during all the sessions. This interval was apparently long enough to prevent temporal sensitization. To evoke equivalent pain in muscle and bone, greater stimulation had to be applied largely to the muscle; this may be because nociceptive nerve density is greater in the periosteum than in muscle [15].

Imaging

A previous positron emission tomography (PET) study and event-related fMRI study using noxious electronic stimulation of muscle showed activation in the ACC, S2, and anterior insula [8, 10]. Also, PET and fMRI study using injection of hypertonic saline into muscle evoked the activation in contralateral insula and putamen [9, 16]. In our study, the results for mechanical stimulation are consistent with the previous muscle pain studies, which have shown that the different types of stimulation (hypertonic saline, electrical stimulation, and mechanical stimulation) applied to muscle induce equivalent activation patterns [8, 10, 16]. We found that stronger muscle stimulation resulted in greater activation in the contralateral S2, the bilateral thalamus (contralateral > ipsilateral), and that stronger bone stimulation caused greater activation in the contralateral S2. In each case, the contralateral S2 was more activated by strong stimulation. However, caution is needed in interpreting these results because greater application of the force to skin is also involved during strong stimulation. The activation of the contralateral S2 may also come from greater cutaneous stimulation. In a PET study investigating thermal stimulation to skin, Coghill et al. [17] have shown that the ipsilateral cerebellum, the contralateral S1, the supplementary motor area, the bilateral S2, the lentiform nucleus, the insular cortex, and the thalamus and ACC are more activated depending on perceived pain intensity. In an fMRI study, using mechanical phasic stimulation on the skin, Ringler et al. [18] have shown that the contralateral S2 is more activated by stronger stimulation. The contralateral S2 may take part in processing pain intensity derived from both skin and deep tissues.

Comparison of the activation associated with muscle and bone stimulation revealed that caudate nucleus and putamen were more activated by muscle than by bone stimulation. No activation existed that was evoked by (bone > muscle) stimulation (data not shown). The activation in these areas is supposed to be related to stimulated sites (muscle or bone), not to stimulation or pain intensity, because these areas were not included as a contrast when we stimulated the single target (muscle or bone) with the

Table 2 Peak coordinates (*x*, *y*, *z*) in Montreal Neurological Institute (MNI) space and Z-scores (>6.00) for the activated brain regions by muscle and bone pain

Region	BA	Muscle pain				BA	Bone pain			
		Peak voxel coordinate			Z-score		Peak voxel coordinate			Z-score
		x	*y*	*z*			*x*	*y*	*z*	
ACC	32	−8	12	44	7.07					
	32	−6	18	32	6.42					
	32	−12	26	30	6.42					
Insula right	13	28	26	2	6.33					
		34	4	8	6.09					
Insula left		−34	6	8	6.25	44	−48	10	6	6.27
	47	−28	24	−8	6.05					
S2 right	40	62	−32	30	6.32					
S2 left	40	−60	−32	28	6.39					
IPL left						40	−48	−52	40	6.57
	40	−48	−58	42	6.33	40	−48	−40	28	6.48
	40	−44	−48	42	6.13	40	−62	−36	32	6.27
Thalamus right		20	−18	10	6.04					
Putamen right		26	2	6	6.16					
		20	−4	8	6.10					
Putamen left		−32	6	6	6.54					
Claustrum left		−26	12	10	6.39		−30	10	6	6.18
Caudate right		16	12	8	6.13					

Brodmann areas are given where available

BA Broadmann area, *ACC* anterior cingulate cortex, *S2* secondary sensory cortex, *IPL* inferior parietal lobule

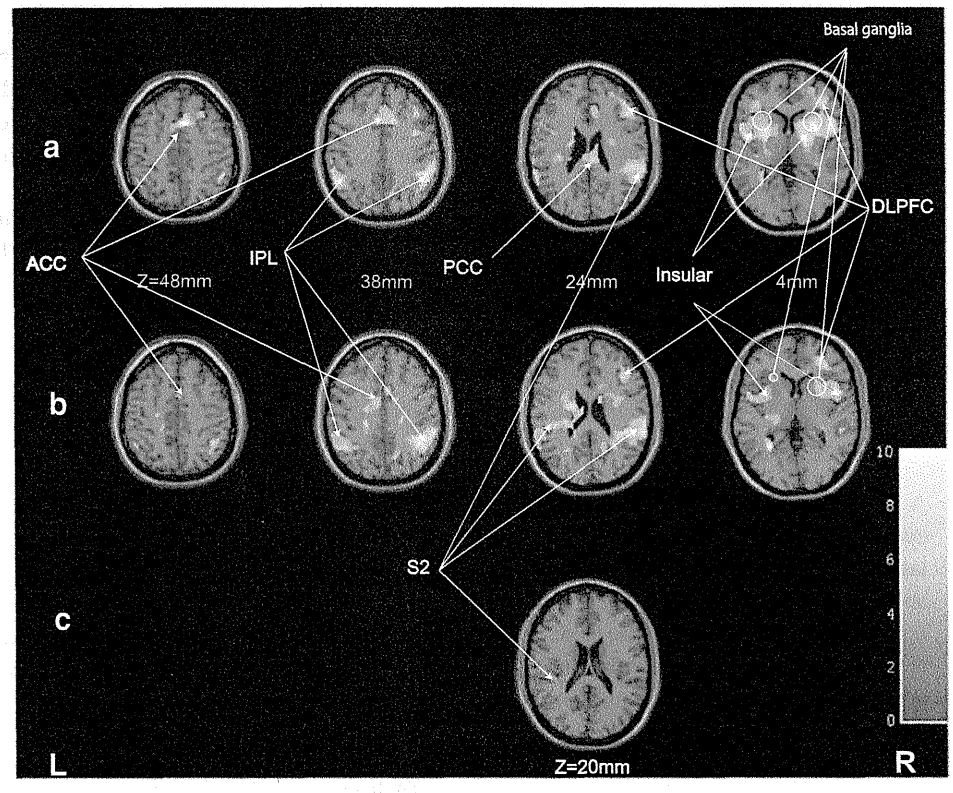

Fig. 4 Brain activation induced by bone stimulation: weak stimulation (**a**), strong stimulation (**b**), and contrast of strong and weak stimulation (**c**). In millimeter elevations relative to a line through the anterior–posterior commissure (AC–PC line), brain slices are shown in superior–inferior sequence. The axial slices are arranged from dorsal (*left*) to ventral (*right*). Statistical map thresholds are $P < 0.001$ (**a**, **b**, uncorrected), and $P < 0.005$ (**c**, uncorrected, paired test). Minimum cluster size is 20 voxels. Right (*R*) and left (*L*) sides are indicated. *ACC* anterior cingulate cortex; *IPL* inferior parietal lobule; *S2* secondary sensory cortex; *DLPFC* dorsolateral prefrontal cortex; *PCC* posterior cingulate cortex

different intensities. Additionally, pain intensities were identical between strong muscle and strong bone pain. Reports of the previous pain imaging studies have suggested that the putamen is activated by nociceptive stimulation [17, 19], including muscle pain with hypertonic saline [16]. Basal ganglia are reported to have a role in

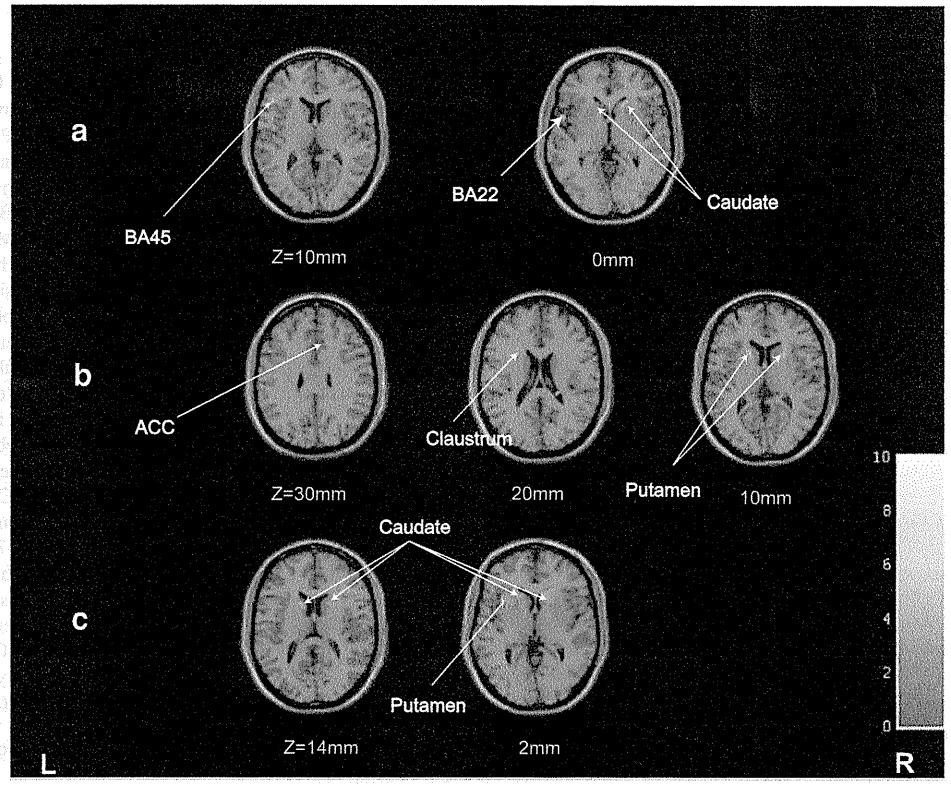

Fig. 5 Contrast of brain activation induced by muscle and bone stimulation: contrast of weak stimulation to muscle and bone (**a**), contrast of strong stimulation to muscle and bone (**b**), and contrast of all the stimulations to muscle and bone (**c**). In millimeter elevations relative to a line through the anterior–posterior commissure (AC–PC line), brain slices are shown in superior–inferior sequence. The axial slices are arranged from dorsal (*left*) to ventral (*right*). Statistical map thresholds are $P < 0.005$ (uncorrected, paired test). Minimum cluster size is 20 voxels. Right (*R*) and left (*L*) sides are indicated. *BA* Brodmann area; *ACC* anterior cingulate cortex

Table 3 Peak coordinates (*x*, *y*, *z*) in Montreal Neurological Institute (MNI) space and *Z*-scores for activated brain regions by muscle–bone pain

Region	(Muscle–bone) pain			
	Peak voxel coordinate			*Z*-score
	x	*y*	*z*	
Putamen left	−24	12	24	4.12
Caudate left	−18	16	8	4.01
Caudate right	16	22	0	3.95

motor preparation, movement control, and emotional, motivational, and cognitive function [20–22]. Processing in the putamen and caudate nucleus is also reported to be related to pain-avoidance behavior [23]. Our results suggest that the putamen and caudate nucleus may have a more significant role in the brain processing of muscle pain compared with bone pain.

Conclusion

In conclusion, the putamen and caudate nucleus may have a more significant role in the brain processing of muscle pain compared to bone pain.

Acknowledgment We thank Syoji Kobashi and Tamotsu Nomura for helping in imaging procedures, Tateo Iwakura for help with image analysis, and Sho Karl Shibata and David Eunice for editing. Scans were performed at Ishikawa Hospital. This work was supported by a Grant-in-aid for community health and medical care from the Ichou Association for Promotion of Medical Science.

Conflict of interest None.

References

1. Hoffman HG, Richards TL, Van Oostrom T, Coda BA, Jensen MP, Blough DK, Sharar SR. The analgesic effects of opioids and immersive virtual reality distraction: evidence from subjective and functional brain imaging assessments. Anesth Analg. 2007;105:1776–83.
2. Buvanendran A, Ali A, Stoub TR, Berger RA, Kroin JS. The use of brain positron emission tomography to identify sites of postoperative pain processing with and without epidural analgesia. Anesth Analg. 2007;105:1784–6.
3. Liu SS, Brown EN. Will seeing become believing? Anesth Analg. 2007;105:1526–7.
4. Lorenz IH, Egger K, Schubert H, Schnurer C, Tiefenthaler W, Hohlrieder M, Schocke MF, Kremser C, Esterhammer R, Ischebeck A, Moser PL, Kolbitsch C. Lornoxicam characteristically modulates cerebral pain-processing in human volunteers: a functional magnetic resonance imaging study. Br J Anaesth. 2008;100:827–33.

5. Kurata J. A potential role of functional magnetic resonance imaging in the diagnosis of pain. Jpn J Anesthesiol. 2009;58: 1350–9. (in Japanese with English abstract).
6. Seifert F, Jungfer I, Schmelz M, Maihofner C. Representation of UV-B-induced thermal and mechanical hyperalgesia in the human brain: a functional MRI study. Hum Brain Mapp. 2008; 29:1327–42.
7. Borsook D, Moulton EA, Tully S, Schmahmann JD, Becerra L. Human cerebellar responses to brush and heat stimuli in healthy and neuropathic pain subjects. Cerebellum. 2007;22:1–21.
8. Niddam DM, Yeh TC, Wu YT, Lee PL, Ho LT, Arendt-Nielsen L, Chen AC, Hsieh JC. Event-related functional MRI study on central representation of acute muscle pain induced by electrical stimulation. Neuroimage. 2002;17:1437–50.
9. Henderson LA, Bandler R, Gandevia SC, Macefield VG. Distinct forebrain activity patterns during deep versus superficial pain. Pain. 2006;120:286–96.
10. Svensson P, Minoshima S, Beydoun A, Morrow TJ, Casey KL. Cerebral processing of acute skin and muscle pain in humans. J Neurophysiol. 1997;78:450–60.
11. Kobayashi Y, Kurata J, Sekiguchi M, Kokubun M, Akaishizawa T, Chiba Y, Konno S, Kikuchi S. Augmented cerebral activation by lumbar mechanical stimulus in chronic low back pain patients: an FMRI study. Spine. 2009;34:2431–6.
12. Gracely RH, Petzke F, Wolf JM, Clauw DJ. Functional magnetic resonance imaging evidence of augmented pain processing in fibromyalgia. Arthritis Rheum. 2002;46:1333–43.
13. Talairach J, Tournoux P. Co-planar stereotactic atlas of the human brain: 3-dimensional proportional system—an approach to cerebral imaging. New York: Thieme; 2002.
14. Nie H, Arendt Nielsen L, Andersen H, Graven Nielsen T. Temporal summation of pain evoked by mechanical stimulation in deep and superficial tissue. J Pain. 2005;6:348–55.
15. Mach DB, Rogers SD, Sabino MC, Luger NM, Schwei MJ, Pomonis JD, Keyser CP, Clohisy DR, Adams DJ, O'Leary P, Mantyh PW. Origins of skeletal pain: sensory and sympathetic innervation of the mouse femur. Neuroscience. 2002;113:155–66.
16. Korotkov A, Radovanovic S, Ljubisavljevic M, Lyskov E, Kataeva G, Roudas M, Pakhomov S, Thunberg J, Medvedev S, Johansson H. Comparison of brain activation after sustained non-fatiguing and fatiguing muscle contraction: a positron emission tomography study. Exp Brain Res. 2005;163:65–74.
17. Coghill RC, Sang CN, Maisog JM, Iadarola MJ. Pain intensity processing within the human brain: a bilateral, distributed mechanism. J Neurophysiol. 1999;82:1934–43.
18. Ringler R, Greiner M, Kohlloeffel L, Handwerker HO, Forster C. BOLD effects in different areas of the cerebral cortex during painful mechanical stimulation. Pain. 2003;105:445–53.
19. Bingel U, Glascher J, Weiller C, Buchel C. Somatotopic representation of nociceptive information in the putamen: an event-related fMRI study. Cereb Cortex. 2004;14:1340–5.
20. Doyon J, Bellec P, Amsel R, Penhune V, Monchi O, Carrier J, Lehericy S, Benali H. Contributions of the basal ganglia and functionally related brain structures to motor learning. Behav Brain Res. 2009;199:61–75.
21. Marchand WR. Cortico-basal ganglia circuitry: a review of key research and implications for functional connectivity studies of mood and anxiety disorders. Brain Struct Funct. 2010;215:73–96.
22. Grahn JA, Parkinson JA, Owen AM. The role of the basal ganglia in learning and memory: neuropsychological studies. Behav Brain Res. 2009;199:53–60.
23. Chudler EH, Dong WK. The role of the basal ganglia in nociception and pain. Pain. 1995;60:3–38.

Neuroscience Research 70 (2011) 78–84

Contents lists available at ScienceDirect

Neuroscience Research

journal homepage: www.elsevier.com/locate/neures

Brain imaging of mechanically induced muscle versus cutaneous pain

Hironobu Uematsu[a,*], Masahiko Shibata[b], Satoru Miyauchi[c,d], Takashi Mashimo[a]

[a] Department of Anesthesiology and Intensive Care Medicine, Osaka University Graduate School of Medicine, 2-2 Yamadaoka, Suita, Osaka 565-0871, Japan
[b] Department of Pain Medicine, Osaka University Graduate School of Medicine, Osaka, Japan
[c] CREST Brain Function Imaging Team, Kobe Advanced ICT Research Center, National Institute of Information and Communications Technology (NICT), Hyogo, Japan
[d] CREST, Japan Science and Technology Agency (JST), Saitama, Japan

ARTICLE INFO

Article history:
Received 12 November 2010
Received in revised form 14 January 2011
Accepted 24 January 2011
Available online 1 February 2011

Keywords:
Functional MRI
Cutaneous pain
Muscle pain
Mechanical stimulation
Local anesthesia
Secondary somatosensory cortex
Insular cortex
Cingulate cortex

ABSTRACT

This study aimed to investigate the differences in the brain responses between muscle versus skin pain, both of which were caused by tonic mechanical stimuli. Using local anesthesia (LA), we induced muscle pain without any accompanying cutaneous sensation. Subjects underwent functional magnetic resonance imaging while tonic pressure was applied to the right calf under the following four conditions: (1) non-painful pressure without LA (causing mechanoreceptive skin and muscle stimulation); (2) painful pressure without LA (causing nociceptive skin stimulation and mechanoreceptive skin and muscle stimulation); (3) non-painful pressure with LA (causing mechanoreceptive muscle stimulation); (4) painful pressure with LA (causing nociceptive and mechanoreceptive muscle stimulation). Although there was no brain region specifically activated by nociceptive muscle stimuli, activation in the following regions was observed specifically during nociceptive muscle stimuli: anterior midcingulate cortex, anterior and posterior insular cortex, lentiform nucleus, thalamus, pre-supplementary motor area, dorsolateral prefrontal cortex, and inferior parietal lobule. This indicates that there is no region specific for muscle pain but activation pattern or network specific for muscle pain. Furthermore, secondary somatosensory cortex (S2) was found to be responsive to cutaneous pain, not muscle pain, because S2 was specifically activated by nociceptive cutaneous stimuli.

1. Introduction

Pathological muscle pain is much more frequently encountered in clinical practice than is superficial cutaneous pain, and its treatment poses a bigger challenge. It has a significant impact on individuals and societies, as well as healthcare services and economies (Suka and Yoshida, 2005). However, the central processing pathways for muscle pain have been less explored than those of cutaneous pain (Sung et al., 2007; Borsook et al., 2008; Seifert et al., 2008). The typical characteristics of pathological muscle pain are mechanical nociception-related pain; i.e., muscle tenderness, pressure and movement-related pain (Staud et al., 2003). As such, studies of mechanically induced muscle pain are required to link the experimental findings from neuroimaging studies with clinical interpretations. Nevertheless, to date there are no functional imaging studies of muscle pain using mechanical stimulation. A classical functional imaging study of muscle pain using phasic electrical stimulation suggested a common representation for both thermally induced cutaneous pain and electrically induced muscle pain (Svensson et al., 1997). More recently, a few studies using tonic muscle stimuli, such as electric stimulation and injection of hypertonic saline or acidic saline, showed distinct temporal activity patterns of the tonic state comparing experimental skin and muscle pain (Schreckenberger et al., 2005; Henderson et al., 2006; Owen et al., 2010). Stimuli such as electric stimulation and injection of hypertonic saline, however, are not physiological energy forms (thermal, mechanical or chemical), and injection of acidic saline includes two forms of stimulus energy (mechanical and chemical). In this regard, studies using such non-physiological stimuli can clarify roles of temporal activity patterns in experimental skin versus muscle pain processing, but only studies using mechanical stimuli can properly link the experimental findings with clinical interpretations.

One of the reasons so few investigators have studied mechanically induced muscle pain is that under normal circumstances, mechanical stimulation to the muscle is always accompanied by cutaneous stimulation (Nie et al., 2005). To resolve this methodological issue, a few recent psychophysical studies used local anesthesia (LA) to stimulate the muscle without any sensation to

Abbreviations: LA, local anesthesia; fMRI, functional magnetic resonance imaging; IPL, inferior parietal lobule; S2, secondary somatosensory cortex; preSMA, pre-supplementary motor area; aMCC, anterior mid-cingulate cortex; aIC, anterior insular cortex; pIC, posterior insular cortex; DLPFC, dorsolateral prefrontal cortex; LN, lentiform nucleus.

* Corresponding author. Tel.: +81 6 6879 3745; fax: +81 6 6879 3495.
E-mail address: Uhironobu@anes.med.osaka-u.ac.jp (H. Uematsu).

0168-0102/$ – see front matter © 2011 Elsevier Ireland Ltd and the Japan Neuroscience Society. All rights reserved.
doi:10.1016/j.neures.2011.01.015

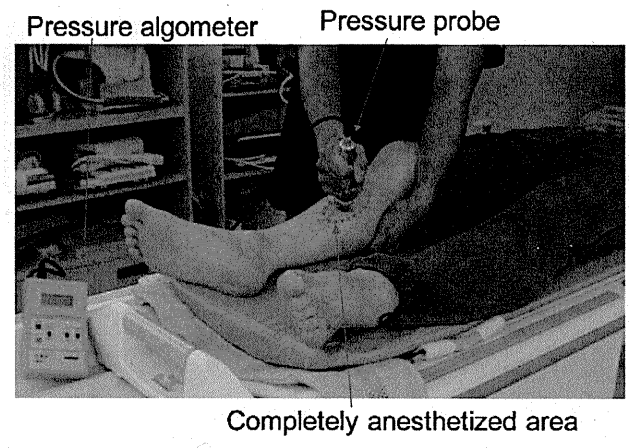

Fig. 1. A pressure probe (diameter, 10 mm) was pressed down perpendicularly to the skin surface over the right calf (gastrocnemius muscle) from the medial side (the periosteum was not stimulated). The experimenter was trained to operate the probe before the experiments so that the pressure was stably maintained and the rate of pressure increase was kept constant. We injected 2 ml of lidocaine (AstraZeneca, Xylocaine® Injection syringe 1%) subcutaneously over the right calf (gastrocnemius muscle) in order to anesthetize the skin completely. We marked the area that was completely anesthetized (at least 3 cm × 3 cm), and all mechanical stimuli were applied in this region.

the skin (Graven-Nielsen et al., 2004; Takahashi et al., 2005). In the present study, we investigated the differences in the brain responses between muscle versus skin pain, both of which were caused by tonic mechanical stimuli, using LA in combination with functional magnetic resonance imaging (fMRI).

2. Materials and methods

2.1. Subjects

Seventeen healthy volunteers (10 males, 7 females, age range 23–33) participated in this study. None of the subjects had any neurological illness or detectable MRI abnormalities. They agreed to receive painful pressure during fMRI scanning. The study was approved by the Osaka University Hospital Institutional Review Board, and written informed consent was obtained from each subject before the experiment. All experiments were conducted in accordance with the Declaration of Helsinki.

2.2. Experimental protocol

A pressure hemispherical probe (diameter, 10 mm) was pressed down perpendicularly to the skin surface over the right calf (gastrocnemius muscle) from the medial side (the periosteum was not stimulated) (Fig. 1). This probe was attached to an electronic pressure algometer (Pressure Algometer NPA-1, Shinko, Japan), which measured the pressure in Newtons (N). The apparatus was held and moved manually. The experimenter was trained to operate the probe before the experiments so that the pressure was stably maintained and the rate of pressure increase was kept constant.

As shown in Table 1, the four experimental conditions were as follows: (A) 10 N pressure *without* LA, causing mechanoreceptive skin and muscle stimulation, but no pain sensation; (B) 20 N pressure *without* LA, causing mechanoreceptive skin and muscle stimulation and pain sensation in skin only; (C) 10 N pressure *with* LA, causing mechanoreceptive muscle stimulation and no pain sensation; and (D) 30 N pressure *with* LA, causing mechanoreceptive and nociceptive muscle stimulation, which resulted in muscle pain without any skin sensation. The pressure intensities in each condition were defined on the basis of the results of the preliminary

Table 1
Four experimental conditions.

Condition	Local anesthesia	Pressure (N)	Pain sensation	Region of painful stimulation	Region of mechanosensory stimulation
A	–	10	–	–	Skin + muscle
B	–	20	+	Skin	Skin + muscle
C	+	10	–	–	Muscle
D	+	30	+	Muscle	Muscle

experiment in which six participants evaluated non-painful and painful sensation in the skin and in the muscle induced by various pressure stimuli (data not shown). The reason why we did not apply the same pressure in Conditions B and D was because some participants were not able to tolerate 30 N pressure without LA in a preliminary experiment. In addition, although the order of Conditions A/B or C/D was pseudo-randomly balanced among all subjects, we performed the conditions without LA (Conditions A and B) before the conditions with LA (Conditions C and D) to avoid the possibility of a lingering effect from the anesthesia.

The experimental paradigm consisted of interleaved rest (40 s) and activation (20 s) phases, leading to a total scanning time of 6 min in each session (7 rest plus 6 activation phases). Time intervals between sessions were at least 1 min, and two sessions were delivered within each condition. There was a 20-s rest period before the first activation, as well as after the last activation, of each session. A total of 8 sessions (48 min) were acquired per subject. The exact location of each probe application was slightly changed throughout the 8 sessions so as not to over-stimulate the same point on the calf.

2.3. Local anesthesia

We injected 2 ml of lidocaine (AstraZeneca, Xylocaine® Injection syringe 1%) subcutaneously over the right calf (gastrocnemius muscle) in order to anesthetize the skin completely, which enabled us to limit stimulation to muscle in Conditions C and D. To assess skin sensation, we applied pin-prick and cold stimuli to the anesthetized skin surface using a stainless steel needle and an 81.4% ethyl alcohol solution. These assessments were performed at least 5 min before and after scanning. We marked the area that was completely anesthetized (at least 3 cm × 3 cm), and all mechanical stimuli were applied in this region.

2.4. Pain intensity rating

The subjective pain intensity was assessed after every session in Conditions B and D. Subjects were asked to rate the mean intensity of pain using a numerical rating scale (NRS) that was defined as follows: 0 = no pain, 10 = worst pain imaginable.

2.5. Functional MRI procedures

A 1.5-T MRI scanner (Signa EXCITE XI 11.0, GE Healthcare, Milwaukee, WI) was used to detect the blood oxygenation level-dependent (BOLD) contrast. fMRI scans were acquired using echo-planar imaging sequences (gradient echo; repetition time [TR], 2500 ms; echo time [TE], 60 ms; flip angle [FA], 90; field of view [FOV], 300 mm; in-plane resolution, 4.69 mm × 4.69 mm; 30 slices of 5 mm thickness, no gap). An interleaved scanning sequence was used. All subjects were positioned in the scanner with a foam rubber pad to minimize head movement and instructed simply to lay with their eyes closed without moving or talking. High-resolution T1-weighted anatomical images with the same orientation as the EPI slices were collected from each subject.

2.6. Data analysis

Statistical parametric mapping (SPM2, Wellcome Department of Cognitive Neurology, London, UK) implemented in Matlab 7 (Mathworks Inc., Sherborn, MA) was used for preprocessing (realignment, normalization, and smoothing [10-mm isotropic Gaussian kernel]; high-pass filter cutoff to 128 s) and statistical analysis of the fMRI data. We used global mean scaling to remove confounding global effects on local signals. To make statistical inferences at the population level, individual data sets were then summarized and incorporated into a random-effects model ($p < 0.005$, uncorrected for multiple comparisons; with cluster size $k > 20$ voxels). To identify statistically significant differences between non-painful and painful conditions, a comparison was conducted with a paired t-test of contrast images ($p < 0.005$, uncorrected for multiple comparisons; with cluster size $k > 20$ voxels): comparison B–A indicates areas showing significant differences in activation in Condition B versus A; comparison D–C indicates areas showing significant differences in activation in Condition D versus C. Since accumulating evidence exists for an *a priori* 'pain matrix' for experimental stimuli (Peyron et al., 2000), we hypothesized that the anatomical structures involved in previous experimental pain were also involved in mechanically induced skin and muscle pain. For the areas with an *a priori* pain-related hypothesis (Svensson et al., 1997; Niddam et al., 2002; Schreckenberger et al., 2005; Henderson et al., 2006; Owen et al., 2010), we applied lenient height and extent thresholds ($p < 0.005$ uncorrected and $k > 20$ (Helmchen et al., 2003; Raij et al., 2005; Moriguchi et al., 2007) within the regions activated in a random-effect analysis and paired t-tests reduced the risk of false negatives. If the regions with the activation and significant differences were included in an *a priori* 'pain matrix' confirmed by previous studies (Svensson et al., 1997; Peyron et al., 2000; Niddam et al., 2002; Schreckenberger et al., 2005; Henderson et al., 2006; Owen et al., 2010), we considered them significant for regionally specific activation and differences associated with mechanically induced skin and muscle pain.

3. Results

3.1. Intensity ratings

The mean pain intensity ratings were as follows: Condition B = 5.8 ± 1.3 (mean ± SEM); Condition D = 4.7 ± 1.7. There were no statistically significant differences in the mean pain intensity ratings between painful Conditions B and D (Wilcoxon's test; $p > 0.05$).

3.2. Brain regions activated by painful stimulation

The common regions activated in all conditions were bilateral pre-supplementary motor area (preSMA), bilateral dorsolateral prefrontal cortex (DLPFC), and bilateral inferior parietal lobule (IPL). Bilateral thalami were activated by painful pressure (Conditions B and D). Bilateral anterior insular (aIC), contralateral posterior insular cortex (pIC), bilateral anterior midcingulate cortex (aMCC) and bilateral lentiform nucleus (LN) were activated in all conditions except Condition C. Bilateral secondary somatosensory cortex (S2) activation was observed in Condition B only (Fig. 2, Table 2).

The S2 (bilateral), pIC (contralateral) and the thalamus (bilateral) were significantly more activated in Condition B than in Condition A (Fig. 2 B–A, Table 3), whereas the aMCC (bilateral), aIC (contralateral) and pIC (contralateral), LN (contralateral), thalamus (bilateral), DLPFC (bilateral), IPL (bilateral) and preSMA (bilateral) were significantly more activated in Condition D than in Condition C (Fig. 2D–C, Table 3).

4. Discussion

In the present study, we used LA in order to anesthetize the skin, which enabled us to mechanically stimulate the muscle without any sensation to the skin, and to directly examined brain responses to mechanically induced muscle pain with fMRI.

4.1. The activation pattern specific to muscle pain

If there are brain regions specifically associated with muscle pain, then they should be specifically activated in Condition D, in which nociceptive stimuli were selectively delivered to the muscle. Although aMCC, aIC, pIC, LN, thalamus, DLPFC, IPL and preSMA were activated in Condition D, these regions were also activated in some other conditions, suggesting that there is no region specific to muscle pain. However, the activation patterns were considerably different across conditions, indicating that while there is no region that specifically processes muscle pain, there may be an activation pattern or network specific to muscle pain. That is, concurrent activation of these multiple regions (aMCC, aIC, pIC, LN, thalamus, DLPFC, IPL and preSMA) could be associated with muscle pain, specifically. In accordance with this idea, Tracey (2005) also suggests that the emergence of pain would not result from the activation of one or more specific brain areas but would emerge from the 'flow and integration of information' among the structures of the Pain Matrix that constitutes, as an ensemble, the neural substrate for pain perception (Tracey, 2005).

Regions activated in Condition D can be divided into two subsets: regions that were not also activated in Condition C (aMCC, aIC and pIC) and regions that were activated in both Conditions C and D (DLPFC, IPL and preSMA). In Condition D, nociceptive stimuli to the muscle were delivered in addition to mechanoreceptive stimuli to the muscle, as were applied in Condition C. Since aMCC, aIC and pIC were activated in Condition D and not activated in Condition C, these regions could be directly associated with muscle pain processing. Previous studies that employed different types of experimental stimuli to the muscle itself (intramuscular injections of hypertonic saline or acidic saline) also suggested that these regions are responsive to muscle pain (Schreckenberger et al., 2005; Henderson et al., 2006; Owen et al., 2010). Further, it was recently reported that the temporal activity patterns in aMCC and aIC are related to muscle pain with the affective response, while that in pIC is responsible for pain intensity rating (Owen et al., 2010). These imply that aMCC, aIC and pIC would be main structures of the activation pattern specific for muscle pain where the affective or sensory-discriminative components of pain perception are implicated. On the other hand, DLPFC, IPL and preSMA were activated in both Conditions C and D. This indicates that these regions are not directly associated with muscle pain processing. In previous studies, these regions did not seem to be the regions directly associated with pain processing, but rather the structures associated with non-specific cognition and multimodal processing (Qiu et al., 2006; Oshiro et al., 2007). Taking all of these results into consideration, muscle pain would result from the concurrent activation of regions directly associated with muscle pain processing (aMCC, aIC and pIC) and regions associated with non-specific cognition or multimodal processing (DLPFC, IPL and preSMA).

4.2. The role of S2 in pain perception

Another notable finding in this study is that S2 was activated in Condition B only. Since it was not possible to mechanically stimulate the skin itself without any sensation to the muscle, S2 activation might have responded to nociceptive skin stimuli and/or mechanoreceptive muscle stimuli. However, S2 was not activated in Conditions C and D, in which LA blocked skin sensation. This

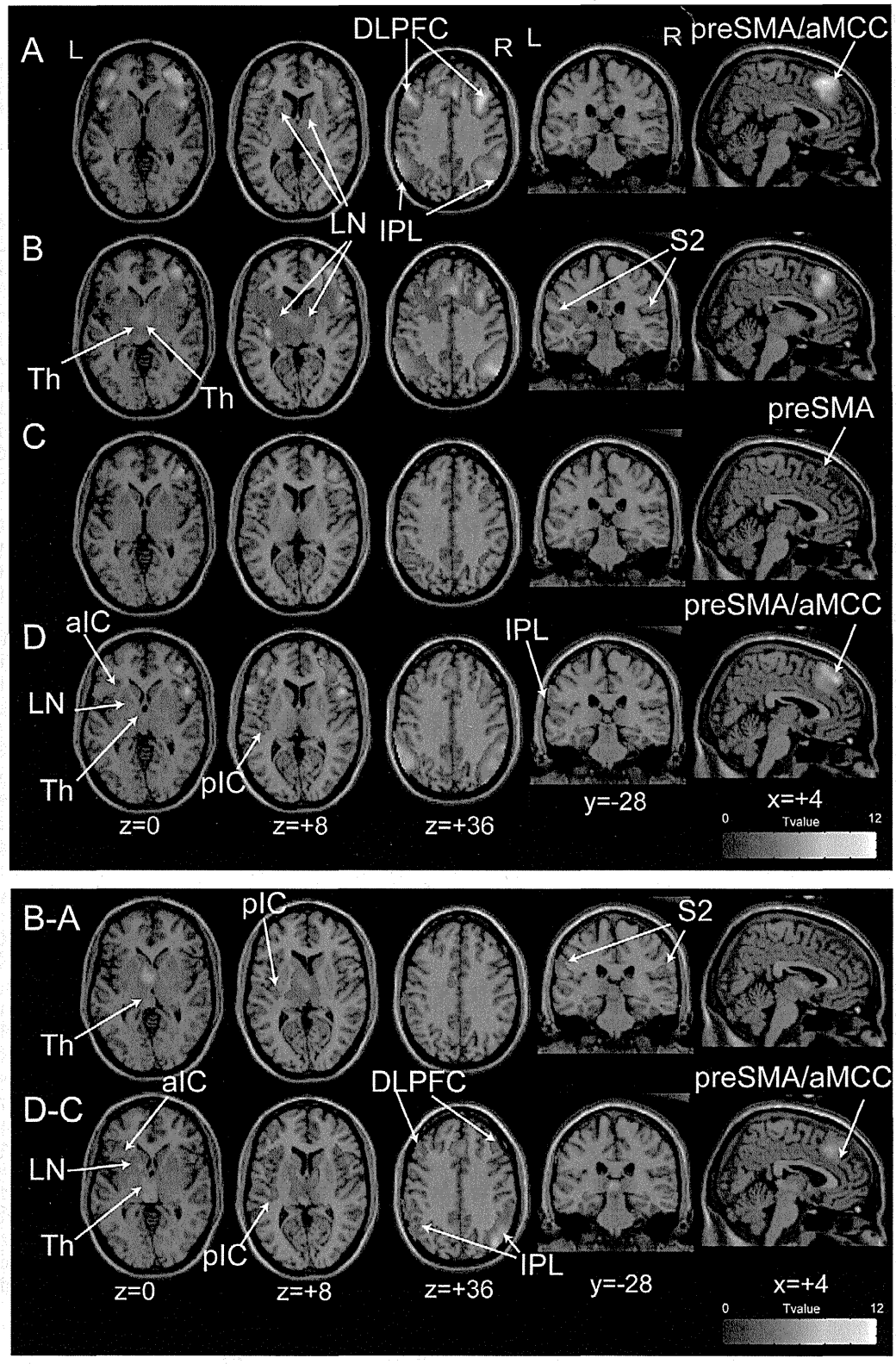

Fig. 2. Panels A–D show the brain regions activated in each condition: A, mechanoreceptive stimuli to skin and muscle (without local anesthesia [LA]); B, nociceptive stimuli to the skin and mechanoreceptive stimuli to the skin and muscle (without LA); C, mechanoreceptive stimuli to the muscle (with LA); D, mechanoreceptive stimuli to the muscle and nociceptive stimuli to the muscle (with LA). Panels B–A show the regions significantly more activated in Condition B than in Condition A. Panels D–C show the regions significantly more activated in Condition D than in Condition C. Activated regions were overlaid on the T1-weighted MNI single-subject template. The color of each activated voxel corresponds to its *T*-value, as per the color bar scales ($n = 17$, height and extent thresholds; $p < 0.005$ uncorrected for multiple comparison and cluster size $k > 20$ voxels). IPL, inferior parietal lobule; S2, secondary somatosensory cortex; preSMA, pre-supplementary motor area; aMCC, anterior mid-cingulate cortex; aIC, anterior insular cortex; pIC, posterior insular cortex; DLPFC, dorsolateral prefrontal cortex; Th, thalamus; LN, lentiform nucleus; L, left side (contralateral to the stimulation); R, right side (ipsilateral to the stimulation).

Table 2
Coordinates (MNI) of regions activated in Conditions A–D.

Region	Condition A				
	Voxels	*x*	*y*	*z*	*T*-value
Right inferior parietal lobule	4115	54	−48	54	10.07
Left inferior parietal lobule	2592	−54	−46	52	9.55
Right pre-supplementary motor area	3275	4	30	54	11.74
Right anterior mid-cingulate cortex		6	26	40	7.13
Left pre-supplementary motor area		−8	28	48	8.40
Left anterior mid-cingulate cortex		−10	22	46	5.27
Right anterior insular cortex	597	38	22	−4	5.22
Left anterior insular cortex	286	−44	14	4	4.69
Left posterior insular cortex	295	−36	−24	8	5.30
Right dorsolateral prefrontal cortex	5382	42	38	24	6.03
Left dorsolateral prefrontal cortex	4065	−50	32	34	6.31
Right lentiform nucleus	329	−12	8	−4	3.99
Left lentiform nucleus	328	−16	12	0	4.04
Region	Condition B				
	Voxels	*x*	*y*	*z*	*T*-value
Right inferior parietal lobule	2016	52	62	38	7.02
Right secondary somatosensory cortex		54	−30	24	5.78
Left inferior parietal lobule	2395	−60	−58	34	6.03
Left secondary somatosensory cortex		−56	−30	22	5.81
Right pre-supplementary motor area	3641	6	32	52	10.07
Right anterior mid-cingulate cortex		6	26	36	6.05
Left pre-supplementary motor area		−8	32	50	7.73
Left anterior mid-cingulate cortex		−4	26	36	5.02
Right anterior insular cortex	608	44	14	4	3.45
Left anterior insular cortex	838	−38	8	8	3.14
Left posterior insular cortex		−34	−20	10	7.31
Right dorsolateral prefrontal cortex	4592	36	16	34	6.73
Left dorsolateral prefrontal cortex	3656	−38	4	38	4.47
Right lentiform nucleus	176	8	2	−2	4.10
Left lentiform nucleus	352	−12	−2	2	3.94
Right thalamus	351	2	−6	6	4.84
Left thalamus	364	−2	−6	6	4.66
Region	Condition C				
	Voxels	*x*	*y*	*z*	*T*-value
Right inferior parietal lobule	852	56	−44	52	5.05
Left inferior parietal lobule	1268	−42	−54	40	4.95
Right pre-supplementary motor area	335	2	18	60	3.21
Left pre-supplementary motor area		−2	18	60	4.44
Right dorsolateral prefrontal cortex	3019	38	20	34	4.01
Left dorsolateral prefrontal cortex	977	−54	20	28	4.08
Region	Condition D				
	Voxels	i	*y*	*z*	*T*-value
Right inferior parietal lobule	2711	46	−66	44	6.81
Left inferior parietal lobule	2898	−64	−48	28	7.66
Right pre-supplementary motor area	2638	2	24	42	6.81
Right anterior mid-cingulate cortex		2	34	32	4.72
Left pre-supplementary motor area		−2	38	50	8.25
Left anterior mid-cingulate cortex		−4	28	36	5.76
Right anterior insular cortex	250	44	14	6	3.82
Left anterior insular cortex	334	−30	18	−6	3.91
Left posterior insular cortex	67	−38	−22	8	4.17
Right dorsolateral prefrontal cortex	3646	40	34	20	6.85
Left dorsolateral prefrontal cortex	2926	−44	38	18	6.99
Left lentiform nucleus	53	−16	10	−6	3.44
Right thalamus	456	4	−12	0	4.15
Left thalamus	79	−4	−14	0	3.50

suggests that S2 is the region specific for mechanically induced cutaneous pain. This notion is supported by the following findings. First, S2 was activated in Condition B and not in Condition D, even though the pressure intensity in Condition D was stronger than that in Condition B. Therefore, the S2 activation does not appear to encode stimulus intensity (Maihofner et al., 2006; Maihofner and Kaltenhauser, 2009). Second, no activation of S2 in Condition A and the significantly stronger activation in Condition B than in Condition A suggest that S2 was activated by nociceptive stimulation, but not by mechanoreceptive stimulation. Last, in previous brain imaging studies, S2 was one of the most consistently activated regions associated with pain limited to the skin and the following: contact heat stimuli (Coghill et al., 1994, 1999; Apkarian et al., 2005), cold stimuli (Davis et al., 2002; Porro et al., 2004) or laser stimuli (Qiu

Table 3
Coordinates (MNI) of the significant differences in Comparison B–A and Comparison D–C.

Region	Comparison B–A				
	Voxels	x	y	z	T-value
Right secondary somatosensory cortex	129	54	−28	26	4.27
Left secondary somatosensory cortex	830	−60	−20	18	8.65
Left posterior insular cortex	59	−36	−16	10	3.54
Right thalamus	273	2	−6	4	5.81
Left thalamus	438	−18	−18	10	3.47
Region	Comparison D–C				
	Voxels	x	y	z	T-value
Right inferior parietal lobule	1651	48	−64	40	6.04
Left inferior parietal lobule	1344	−48	−64	44	5.06
Right pre-supplementary motor area	2071	2	28	42	6.18
Right anterior mid-cingulate cortex		6	34	32	4.36
Left pre-supplementary motor area		−8	26	44	6.45
Left anterior mid-cingulate cortex		−4	28	36	4.38
Left anterior insular cortex	327	−28	20	−4	4.03
Left posterior insular cortex	138	−36	−22	8	4.09
Right dorsolateral prefrontal cortex	1358	40	34	20	4.32
Left dorsolateral prefrontal cortex	1378	−46	32	24	4.84
Right lentiform nucleus	49	14	2	10	4.46
Left lentiform nucleus	263	−12	4	2	4.63
Right thalamus	250	4	14	0	4.79
Left thalamus	411	−6	−26	4	4.79

et al., 2006). On the other hand, a few studies using intramuscular electrical stimulation (IMES) reported that S2 is activated by muscle pain (Svensson et al., 1997; Niddam et al., 2002). The inconsistency may be derived from the inappropriate use of IMES for muscle-specific stimulation (Niddam and Hsieh, 2009). That is, IMES may stimulate both muscle and skin nerve fibers because of its high intensity to induce pain sensation. In addition, muscle and skin twitches accompany IMES. Considering these issues, the pressure stimulation applied in our study shows that S2 is an area specific for cutaneous pain, but not for muscle pain.

4.3. The thalamus

The thalamus was activated in Conditions B and D, in which a nociceptive stimulus was delivered to the skin or the muscle. Since the thalamus is a critical part of the pain matrix, the activation of the thalamus would be associated with pain perception, irrespective of whether the skin or the muscle was stimulated. Another possibility is that the nociceptive stimulus changed the arousal level or non-specific attention (Portas et al., 1998) and the thalamus was thereby activated in Conditions B and D.

4.4. Limitation

The primary somatosensory cortex (S1) was not activated under any conditions in this study using somatosensory mechanical stimuli to the lower leg. Although the reason for the absence of S1 activation is not clear, the most likely explanation seems to be the small somatotopic representation of the lower leg in S1 and the pin head sized stimulation employed in the present study. It is well known that S1 is somatotopically organized and the size of the area representing the lower leg is much smaller than that of the hand (Penfield and Boldrey, 1937). A previous fMRI study, in which thermal stimuli were also applied to the lower leg, reported the absence of activation in S1 by somatosensory stimuli (Oshiro et al., 2007). Therefore, S1 activation by somatosensory stimulation to the calf was not detected, probably because of its small somatotopic mapping.

We did not assess the affective and discriminative components of pain processing, nor did we use graded mechanical stimuli to identify a brain mechanism that encodes stimulus intensity. Instead, we focused on clarifying distinct brain responses by mechanically induced skin versus muscle pain in this study. Therefore, we do not have adequate data to further speculate about the encoding of stimulus intensity or detection and recognition of the noxious nature of nociceptive stimuli.

5. Conclusion

Our results show distinct brain responses to mechanically induced muscle versus skin pain using local anesthesia, which enabled us to induce muscle pain without any accompanying sensation to the skin. We found that the combined activations of aMCC, aIC, pIC, LN, thalamus, DLPFC, IPL and preSMA create a pattern specific for mechanically induced muscle pain, although none of these regions alone seems to be specific for muscle pain. Furthermore, S2 was shown to be an area specific for cutaneous pain but not for muscle pain. These findings reveal a divergence in the pathways for processing tonic muscle and skin pain, and shed light on the neural pathways underlying processing of muscle pain.

Acknowledgements

We thank Tamotsu Nomura for help with imaging procedures, Shigeyuki Kan, Takahiko Koike, Yoshiki Maeda and Yoshitetsu Oshiro for help with image analysis and editing, and Tetsuo Koyama, Masahiko Sumitani and Jeri Helen for manuscript editing. Scans were performed at Ishikawa Hospital.

References

Apkarian, A.V., Bushnell, M.C., Treede, R.D., Zubieta, J.K., 2005. Human brain mechanisms of pain perception and regulation in health and disease. Eur. J. Pain 9, 463–484.

Borsook, D., Moulton, E.A., Tully, S., Schmahmann, J.D., Becerra, L., 2008. Human cerebellar responses to brush and heat stimuli in healthy and neuropathic pain subjects. Cerebellum 7, 252–272.

Coghill, R.C., Talbot, J.D., Evans, A.C., Meyer, E., Gjedde, A., Bushnell, M.C., Duncan, G.H., 1994. Distributed processing of pain and vibration by the human brain. J. Neurosci. 14, 4095–4108.

Coghill, R.C., Sang, C.N., Maisog, J.M., Iadarola, M.J., 1999. Pain intensity processing within the human brain: a bilateral, distributed mechanism. J. Neurophysiol. 82, 1934–1943.

Davis, K.D., Pope, G.E., Crawley, A.P., Mikulis, D.J., 2002. Neural correlates of prickle sensation: a percept-related fMRI study. Nat. Neurosci. 5, 1121–1122.
Graven-Nielsen, T., Mense, S., Arendt-Nielsen, L., 2004. Painful and non-painful pressure sensations from human skeletal muscle. Exp. Brain Res. 159, 273–283.
Helmchen, C., Mohr, C., Erdmann, C., Petersen, D., Nitschke, M.F., 2003. Differential cerebellar activation related to perceived pain intensity during noxious thermal stimulation in humans: a functional magnetic resonance imaging study. Neurosci. Lett. 335, 202–206.
Henderson, L.A., Bandler, R., Gandevia, S.C., Macefield, V.G., 2006. Distinct forebrain activity patterns during deep versus superficial pain. Pain 120, 286–296.
Maihofner, C., Herzner, B., Otto Handwerker, H., 2006. Secondary somatosensory cortex is important for the sensory-discriminative dimension of pain: a functional MRI study. Eur. J. Neurosci. 23, 1377–1383.
Maihofner, C., Kaltenhauser, M., 2009. Quality discrimination for noxious stimuli in secondary somatosensory cortex: a MEG-study. Eur. J. Pain 13, 1048, e1-1048.e7.
Moriguchi, Y., Decety, J., Ohnishi, T., Maeda, M., Mori, T., Nemoto, K., Matsuda, H., Komaki, G., 2007. Empathy and judging other's pain: an fMRI study of alexithymia. Cereb. Cortex 17, 2223–2234.
Niddam, D.M., Yeh, T.C., Wu, Y.T., Lee, P.L., Ho, L.T., Arendt-Nielsen, L., Chen, A.C., Hsieh, J.C., 2002. Event-related functional MRI study on central representation of acute muscle pain induced by electrical stimulation. Neuroimage 17, 1437–1450.
Niddam, D.M., Hsieh, J.C., 2009. Neuroimaging of muscle pain in humans. J. Chin. Med. Assoc. 72, 285–293.
Nie, H., Arendt-Nielsen, L., Andersen, H., Graven-Nielsen, T., 2005. Temporal summation of pain evoked by mechanical stimulation in deep and superficial tissue. J. Pain 6, 348–355.
Oshiro, Y., Quevedo, A.S., McHaffie, J.G., Kraft, R.A., Coghill, R.C., 2007. Brain mechanisms supporting spatial discrimination of pain. J. Neurosci. 27, 3388–3394.
Owen, D.G., Clarke, C.F., Ganapathy, S., Prato, F.S., St Lawrence, K.S., 2010. Using perfusion MRI to measure the dynamic changes in neural activation associated with tonic muscular pain. Pain 148, 375–386.
Penfield, W., Boldrey, E., 1937. Somatic motor and sensory representation in the cerebral cortex of man as studied by electrical stimulation. Brain 60, 389–443.
Peyron, R., Laurent, B., Garcia-Larrea, L., 2000. Functional imaging of brain responses to pain. A review and meta-analysis (2000). Neurophysiol. Clin. 30, 263–288.
Porro, C.A., Lui, F., Facchin, P., Maieron, M., Baraldi, P., 2004. Percept-related activity in the human somatosensory system: functional magnetic resonance imaging studies. Magn. Reson. Imaging 22, 1539–1548.
Portas, C.M., Rees, G., Howseman, A.M., Josephs, O., Turner, R., Frith, C.D., 1998. A specific role for the thalamus in mediating the interaction of attention and arousal in humans. J. Neurosci. 18, 8979–8989.
Qiu, Y., Noguchi, Y., Honda, M., Nakata, H., Tamura, Y., Tanaka, S., Sadato, N., Wang, X., Inui, K., Kakigi, R., 2006. Brain processing of the signals ascending through unmyelinated C fibers in humans: an event-related functional magnetic resonance imaging study. Cereb. Cortex 16, 1289–1295.
Raij, T.T., Numminen, J., Narvanen, S., Hiltunen, J., Hari, R., 2005. Brain correlates of subjective reality of physically and psychologically induced pain. Proc. Natl. Acad. Sci. U.S.A. 102, 2147–2151.
Schreckenberger, M., Siessmeier, T., Viertmann, A., Landvogt, C., Buchholz, H.G., Rolke, R., Treede, R.D., Bartenstein, P., Birklein, F., 2005. The unpleasantness of tonic pain is encoded by the insular cortex. Neurology 64, 1175–1183.
Seifert, F., Jungfer, I., Schmelz, M., Maihofner, C., 2008. Representation of UV-B-induced thermal and mechanical hyperalgesia in the human brain: a functional MRI study. Hum. Brain Mapp. 29, 1327–1342.
Staud, R., Cannon, R.C., Mauderli, A.P., Robinson, M.E., Price, D.D., Vierck Jr., C.J., 2003. Temporal summation of pain from mechanical stimulation of muscle tissue in normal controls and subjects with fibromyalgia syndrome. Pain 102, 87–95.
Suka, M., Yoshida, K., 2005. Musculoskeletal pain in Japan: prevalence and interference with daily activities. Mod. Rheumatol. 15, 41–47.
Sung, E.J., Yoo, S.S., Yoon, H.W., Oh, S.S., Han, Y., Park, H.W., 2007. Brain activation related to affective dimension during thermal stimulation in humans: a functional magnetic resonance imaging study. Int. J. Neurosci. 117, 1011–1027.
Svensson, P., Minoshima, S., Beydoun, A., Morrow, T.J., Casey, K.L., 1997. Cerebral processing of acute skin and muscle pain in humans. J. Neurophysiol. 78, 450–460.
Takahashi, K., Taguchi, T., Itoh, K., Okada, K., Kawakita, K., Mizumura, K., 2005. Influence of surface anesthesia on the pressure pain threshold measured with different-sized probes. Somatosens. Mot. Res. 22, 299–305.
Tracey, I., 2005. Nociceptive processing in the human brain. Curr. Opin. Neurobiol. 15, 478–487.

Factors Predicting Requirement of High-dose Transdermal Fentanyl in Opioid Switching From Oral Morphine or Oxycodone in Patients With Cancer Pain

Yuko Kanbayashi, PhD, BCOPS,†‡ Toyoshi Hosokawa, MD, PhD,*§ Kousuke Okamoto, PhD,‡ Sawako Fujimoto, CN,* Hideyuki Konishi, MD, PhD,‖ Eigo Otsuji, MD, PhD,¶ Toshikazu Yoshikawa, MD, PhD,‖ Tatsuya Takagi, PhD,‡# Tsuneharu Miki, MD, PhD,** and Masafumi Taniwaki, MD, PhD††*

Objectives: To identify predictive factors requiring high-dose transdermal fentanyl in opioid switching from oral morphine or oxycodone to transdermal fentanyl in patients with cancer pain.

Methods: The participants were 76 hospitalized terminal cancer patients who underwent opioid switching from oxycodone or morphine sustained-release tablet to transdermal fentanyl at our hospital between January 2009 and June 2010. The conversion dose was calculated as transdermal fentanyl (25 μg/h)/oral morphine (60 mg) or oxycodone (40 mg) = 1. The response evaluated was the dose conversion ratio [transdermal fentanyl/oral morphine or oxycodone (conversion dose to fentanyl)] = Y and was taken to be 0 for $Y \leq 1$, 1 for $1 < Y \leq 2$, 2 for $2 < Y \leq 3$, and 3 for $3 < Y$. Predictors evaluated were factors potentially impacting pain. Ordered logistic regression analysis was carried out to identify the predictive factors requiring high-dose transdermal fentanyl in opioid switching.

Results: Breast cancer [odds ratio (OR) = 8.218; 95% confidence interval (CI), 1.219-55.407; $P = 0.0305$], total protein level (OR = 0.630; 95% CI, 0.408-0.974; $P = 0.0377$), alanine aminotransferase level (OR = 1.017; 95% CI, 1.001-1.033; $P = 0.0390$), advanced age (OR = 3.700; 95% CI, 1.360-10.063; $P = 0.0104$), and male sex (OR = 3.702; 95% CI, 1.355-10.115; $P = 0.0107$) were found to be significant predictive factors requiring high-dose transdermal fentanyl in opioid switching.

Discussion: Our study indicates that breast cancer, total protein, alanine aminotransferase, advanced age, and male sex are significant predictors of a need for higher dose transdermal fentanyl in opioid switching. Our results are considered likely to contribute to the establishment of evidence-based medicine in pain relief and palliative care.

Key Words: transdermal fentanyl, opioid switching, morphine, oxycodone, cancer pain

(*Clin J Pain* 2011;27:664–667)

Transdermal fentanyl has recently come into common use in patients with cancer pain because of its excellent side effect profile and ease of application.[1–5] Many patients who do not achieve sufficient pain control with transdermal fentanyl, however, fail to attain satisfactory analgesic effect when the dose is increased.[6–8] Such patients may enjoy satisfactory pain control when switched to a morphine or oxycodone product (opioid switching).[8] Patients conversely undergoing opioid switching from an oral morphine or oxycodone product to transdermal fentanyl because of difficulty swallowing may require a higher fentanyl dose than the recommended conversion dose.[9] This has been attributed to terminal cancer patients being unable to absorb substances transdermally and to healthy persons,[10] but the exact causes have not been elucidated. We, therefore, planned this research with the realization that identifying predictive factors requiring high-dose transdermal fentanyl in opioid switching from oral morphine or oxycodone to transdermal fentanyl in patients with cancer pain would help to establish evidence-based medicine for better treatment of cancer pain.

PATIENTS AND METHODS

Study Term and Participants

Patient care records were searched to identify 76 hospitalized terminal cancer patients who underwent opioid switching from oxycodone or morphine-sustained release tablet to transdermal fentanyl at the University Hospital of Kyoto Prefectural University of Medicine between January 2009 and June 2010. This study was carried out with the approval of the ethics review boards of Kyoto Prefectural University of Medicine and Osaka University.

Data Collection

The conversion dose was calculated as transdermal fentanyl (25 μg/h)/oral morphine (60 mg) or oxycodone (40 mg) = 1.[9] The response evaluated was the dose conversion ratio [transdermal fentanyl/oral morphine or oxycodone (conversion dose to fentanyl)] = Y and was taken to be 0 for $Y \leq 1$, 1 for $1 < Y \leq 2$, 2 for $2 < Y \leq 3$, and 3 for $3 < Y$. We extracted the dosage of the following transdermal fentanyl on the opioid switching day 7. Predictors evaluated were factors potentially impacting pain [sex, age, sites of metastasis, body mass index, laboratory test values, and

Received for publication December 12, 2010; revised February 5, 2011; accepted February 19, 2011.

From the Departments of *Pain Treatment and Palliative Care Unit; †Hospital Pharmacy, University Hospital, Kyoto Prefectural University of Medicine; Departments of §Anaesthesiology; ‖Molecular Gastroenterology and Hepatology; ¶Digestive Surgery; **Urology; ††Molecular Hematology and Oncology, Kyoto Prefectural University of Medicine, Graduate School of Medical Science, Kyoto; ‡Pharmainformatics and Pharmacometrics, Graduate School of Pharmaceutical Sciences; and #Genome Information Research Center, Research Institute for Microbial Diseases, Osaka University, Suita, Japan.

The authors declare no conflict of interest.

Reprints: Yuko Kanbayashi, PhD, Department of Hospital Pharmacy, Kyoto Prefectural University of Medicine, Kawaramachi Hirokoji, Kamigyo-ku, Kyoto 602-8566, Japan (e-mail: ykokanba@koto.kpu-m.ac.jp).

cancer type]. Laboratory tests that relate to nutritional status, medical condition, hepatic function, and renal function that seemed to influence pain or absorption and pharmacological effects of the transdermal fentanyl were extracted. The retrospective nature of this study made accurate determination of the skin condition of patients difficult, therefore body mass index, which typically decreases as cancer progresses, and nutrition [serum albumin and total protein (TP) levels] were used as alternative indicators of skin condition.

Statistical Analysis

The analytical procedure used was ordered logistic regression, as dose conversion ratio (= response Y) was rated using a graded scale and multiple factors potentially involved in the predictive factors requiring high-dose transdermal fentanyl in opioid switching (= predictors X) had to be evaluated simultaneously. Variables that were highly intercorrelated (correlation coefficient, $r > 0.7$) were excluded because of multicolinearity, which occurs when correlations exist among variables and results in the use of an inappropriate model. One of variables was selected in consideration of correlation strength with response Y or clinical use. A multivariate logistic regression model was constructed using forward stepwise selection among several candidate variables with a variable entry criterion of 0.25 and a variable retention criterion of 0.1. Variables were further screened with the forward selection procedure, after which ordered logistic regression analysis was carried out with the selected variables (JMP 8 software; SAS Institute, Cary, NC). For all statistical analyses, values of $P < 0.05$ (2-tailed) were considered significant.

RESULTS

Table 1 shows characteristics and factors extracted from the 76 patients that may affect doses of transdermal fentanyl in opioid switching. Reasons for switching were difficulty swallowing in 50 patients, nausea/vomiting in 17, drowsiness in 5, decline of renal function in 2, and delirium and intestinal obstruction in 1 patient, respectively. Table 2 shows the conversion ratio in 76 patients, and the 4 categories used. Breast cancer, TP, serum creatinine, bilirubin, alanine aminotransferase (ALT), age, and sex were extracted by forward selection. When multivariate ordered logistic regression analysis was carried out using these variables, breast cancer{[odds ratio (OR) = 8.218; 95% confidence interval (CI), 1.219-55.407; $P = 0.0305$]}TP level (OR = 0.630; 95% CI, 0.408-0.974; $P = 0.0377$). ALT level (OR = 1.017; 95% CI, 1.001-1.033; $P = 0.0390$), advanced age (OR = 3.700; 95% CI, 1.360-10.063; $P = 0.0104$), and male sex (OR = 3.702; 95% CI, 1.355-10.115; $P = 0.0107$) were found to be significant predictors requiring high-dose transdermal fentanyl in opioid switching (Table 3).

TABLE 1. Patient Characteristics and Extracted Factors That May Affect Pain (n=76)

	n (%)	Mean ± SD	Range
Demographic factors			
Sex, (male)	42 (55.3)		
Age, years (≥ 65 y)	38 (50.0)	62.9 ± 14.6	8-85
Physical examination findings			
Bone metastasis	31 (40.8)		
Lymph node metastasis	43 (56.6)		
Peritoneal dissemination	16 (21.1)		
Organ metastasis	41 (53.9)		
BMI		21.0 ± 3.76	12.11-32.76
Laboratory test			
CRP, mg/dL		6.41 ± 6.38	0.03-29.79
ALT, U/L		37.3 ± 62.5	5-492
Albumin, g/dL		2.93 ± 0.62	1.7-4.4
Bilirubin, mg/dL		0.29 ± 0.68	0.14-11.48
Serum creatinine, mg/dL		0.90 ± 0.63	0.16-3.39
Total protein, mg/dL		6.06 ± 1.07	3.9-12.1
Hemoglobin, g/dL		9.13 ± 2.13	4.6-14.8
Daily dosage of opioid			
Oral morphine, mg (n = 5)		30.00 ± 14.14	20-50
Oral oxycodone, mg (n = 71)		26.41 ± 17.99	5-80
Transdermal fentanyl, μg/h (n = 76)		4.64 ± 2.44	1.05-12.6
Type of cancer			
Lung	11 (14.5)		
Gastric	10 (13.2)		
Myeloma	5 (6.6)		
Breast	5 (6.6)		
Colon	4 (5.3)		
Pancreas	4 (5.3)		
Ovarian	4 (5.3)		
Pharyngeal	4 (5.3)		
Esophageal	3 (3.9)		
Melanoma	3 (3.9)		
Bladder	3 (3.9)		
Renal pelvic	3 (3.9)		
Liver	2 (2.6)		
Cholangiocarcinoma	2 (2.6)		
Lymphoma	2 (2.6)		
Renal cellular	2 (2.6)		
Others	9 (11.8)		

ALT indicates alanine aminotransferase; BMI, body mass index; CRP, C-reactive protein.

DISCUSSION

Factors predicting a need for high-dose transdermal fentanyl in opioid switching from oral morphine or oxycodone among patients with cancer pain were breast cancer, TP, high ALT, advanced age, and male sex. Earlier research identified differences in transdermal fentanyl absorption for different diseases.[11,12] Solassol et al[12] stated that there was a significant difference in the percentage of absorbed fentanyl according to the type of cancer and absorption was higher in patients with breast or digestive cancer than in those with lung cancer. In contrast, our study found that breast cancer patients required high-dose transdermal fentanyl when undergoing opioid switching. Patients with advanced breast cancer frequently develop metastasis to bone. Bone metastasis results in intractable pain.[13,14] Breast cancer patients may, therefore, not respond well to fentanyl. This study did not identify metastasis site as a predictive factor. We intend to investigate differences in responses to fentanyl for patients with different diseases further.

TP and ALT were identified as laboratory findings predicting a need for high-dose transdermal fentanyl. Heiskanen et al[10] stated with regard to low TP levels, that

TABLE 2. Categorization of Dose Conversion Ratio

Response (Y)	Dose-conversion Ratio	n (N = 76)
0	$Y \leq 1$	16
1	$1 < Y \leq 2$	37
2	$2 < Y \leq 3$	9
3	$3 < Y$	14

The response evaluated was the dose conversion ratio [transdermal fentanyl/oral morphine or oxycodone (conversion dose to fentanyl)] = Y and was taken to be 0 for $Y \leq 1$, 1 for $1 < Y \leq 2$, 2 for $2 < Y \leq 3$, and 3 for $3 < Y$.

is, poor nutrition. that patients with far advanced cancer often suffered from cachexia. which might have negative effects on the absorption of transdermal fentanyl. The findings in our study agree with earlier research finding that transdermal fentanyl absorption is poor in patients with cachexia. Moreover. fentanyl is metabolized by the drug-metabolizing enzyme CYP3A4 present in the liver, and therefore must be used with care when given in combination with CYP3A4 inhibitors, as such combinations have been shown to result in elevated blood concentrations.[15–17] Other studies. however, have found that the efficacy of fentanyl is unaffected by liver disease[18] and that fentanyl drug sensitivity differs among individuals.[19] The effects of high ALT levels and other liver function markers on response to fentanyl must be further clarified.

Advanced age was identified as a predictive factor. Earlier research has also found that transdermal fentanyl absorption worsens with advancing age.[12,20,21] Decreasing moisture content of the skin with aging is thought to decrease transdermal fentanyl absorption. Solassol et al[12] stated that bioavailability of fentanyl differed significantly according to patient age. Patients older than 75 years absorbed 50% of the fentanyl during the selected 72-hour period, whereas patients younger than 65 years absorbed 66%. Our results support those findings.

Male sex was identified as a predictive factor. As for cancer pain, an earlier study clarified that pain was significantly exacerbated when the patient was male.[14] Gupta et al,[22] however, found no sex-based differences in transdermal fentanyl absorption. Yet, other studies have stated that women absorb transdermal fentanyl less effectively and require higher doses because of higher levels of subcutaneous fat.[23] The impact of sex requires further characterization.

TABLE 3. Results of Ordered Logistic Regression Analysis for Variables Extracted by Forward Selection (Accuracy=45/76)

Variable	P	Odds Ratio	CI of Odds Ratio	
			Lower 95%	Upper 95%
Breast cancer	0.0305*	8.218	1.219	55.407
TP	0.0377*	0.630	0.408	0.974
sCr	0.1123	0.546	0.258	1.1525
T-bil	0.18	0.822	0.618	1.095
ALT	0.0390*	1.017	1.001	1.033
Age	0.0104*	3.700	1.360	10.063
Sex	0.0107*	3.702	1.355	10.115

*$P < 0.05$.

ALT indicates alanine aminotransferase; CI, confidence interval; sCr, serum creatinine; T-bil, total bilirubin; TP, total protein.

In conclusion, we used a statistical approach to identify factors predicting a need for higher dose transdermal fentanyl in opioid switching from oral morphine or oxycodone in patients with cancer pain. Our study indicates that breast cancer, TP. ALT, advanced age, and male sex are significant predictors of a need for higher dose transdermal fentanyl in opioid switching. Our study has limitations in terms of the retrospective nature of the investigation and the relatively small number of patients analyzed. 95% CI shows a very wide range especially in breast cancer, so our results have a limitation in precision. But the statistical identification of predictors for higher dose transdermal fentanyl in opioid switching is considered likely to contribute to the establishment of evidence-based medicine in pain relief and palliative care.

REFERENCES

1. Radbruch L, Sabatowski R, Loick G, et al. Constipation and the use of laxatives: a comparison between transdermal fentanyl and oral morphine. *Palliat Med.* 2000;14:111–119.
2. Ripamonti C, Fagnoni E, Campa T, et al. Is the use of transdermal fentanyl inappropriate according to the WHO guidelines and the EAPC recommendations? A study of cancer patients in Italy. *Support Care Cancer.* 2006;14:400–407.
3. Morita T, Takigawa C, Onishi H, et al. Opioid rotation from morphine to fentanyl in delirious cancer patients: an open-label trial. *J Pain Symptom Manage.* 2005;30:96–103.
4. Allan L, Hays H, Jensen NH, et al. Randomised crossover trial of transdermal fentanyl and sustained release oral morphine for treating chronic non-cancer pain. *BMJ.* 2001;322:1154–1158.
5. Menten J, Desmedt M, Lossignol D, et al. Longitudinal follow-up of TTS fentanyl use in patients with cancer-related pain: results of a compassionate use study with special focus on elderly patients. *Curr Med Res Opin.* 2002;18:488–498.
6. Benítez-Rosario MA, Feria M, Salinas-Martín A, et al. Opioid switching from transdermal fentanyl to oral methadone in patients with cancer pain. *Cancer.* 2004;101:2866–2873.
7. Mercadante S, Ferrera P, Villari P, et al. Rapid switching between transdermal fentanyl and methadone in cancer patients. *J Clin Oncol.* 2005;23:5229–5234.
8. Clemens KE, Klaschik E. Clinical experience with transdermal and orally administered opioids in palliative care patients—a retrospective study. *Jpn J Clin Oncol.* 2007;37:302–309.
9. Donner B, Zenz M, Tryba M, et al. Direct conversion from oral morphine to transdermal fentanyl: a multicenter study in patients with cancer pain. *Pain.* 1996;64:527–534.
10. Heiskanen T, Mätzke S, Haakana S, et al. Transdermal fentanyl in cachectic cancer patients. *Pain.* 2009;144:218–222.
11. Van Nimmen NF, Poels KL, Menten JJ, et al. Fentanyl transdermal absorption linked to pharmacokinetic characteristics in patients undergoing palliative care. *J Clin Pharmacol.* 2010;50:667–678.
12. Solassol I, Caumette L, Bressolle F, et al. Inter- and intra-individual variability in transdermal fentanyl absorption in cancer pain patients. *Oncol Rep.* 2005;14:1029–1036.
13. Cicek M, Oursler MJ. Breast cancer bone metastasis and current small therapeutics. *Cancer Metastasis Rev.* 2006;25:635–644.
14. Kanbayashi Y, Okamoto K, Ogaru T, et al. Statistical validation of the relationships of cancer pain relief with various factors using ordered logistic regression analysis. *Clin J Pain.* 2009;25:65–72.
15. Armstrong SC, Wynn GH, Sandson NB. Pharmacokinetic drug interactions of synthetic opiate analgesics. *Psychosomatics.* 2009;50:169–176.
16. Saari TI, Laine K, Neuvonen M, et al. Effect of voriconazole and fluconazole on the pharmacokinetics of intravenous fentanyl. *Eur J Clin Pharmacol.* 2008;64:25–30.